



EVALUATION OF SPECIFIC METHODS TO DETECT CRACK AND DAMAGE OF MECHANICAL BEAM STRUCTURES USING FREE VIBRATION ANALYSIS

Dr.Nabil H. H

University of Baghdad
College of Eng.

Iqbal A. R.

ABSTRACT

The importance of the beam in the service of our life and how the damaged beam costly influence the economy and even endanger the human life itself, draws our attention to study the specific methods to detect crack and damage by using free vibration analysis of mechanical beam structures. In the present research, three kinds of beam structures have been investigated namely (simply supported beam, portal frame and crane frame) by using finite element method. Six cases of damage are modeled for simply supported beam and portal frame and with seven cases for crane frame. The damage is simulated by reducing the stiffness of assumed elements with ratios (25% and 50 %) in mid- span of the simply supported beam and by introducing cracked elements at different locations with ratio of depth of crack to the height of the beam (a/h) 0.1, 0.25 for simply supported beam and 0.1 and 0.2 for portal and crane frames. A program coded in Matlab 6.5 was used to model the numerical simulation of the damage scenarios. The results showed a decreasing in the five natural frequencies with shifting in the damaged mode shape associated with their frequencies from undamaged beam which means the indication of presence of the damage. The direct comparison gives an indication of the damage but the location of the damage, is not detected. Four structural damage identification methods based on changes in the dynamics characteristics of the beam structures are examined and evaluated for damage scenarios for the three structures considered. The results of the analysis indicate that the curvature energy damage index method performs well in detecting, locating and quantifying damage in single and multiple damage scenarios for the three structures.

الخلاصة

نظرا لأهمية العتبة beam في خدمة حياتنا ، فإن العتبة المتضررة تؤثر سلبا على الاقتصاد بل وتهدد حياة الانسان نفسها مما جذب اهتمامنا نحو دراسة طرق معينة لتحديد الشق و الضرر باستخدام الاهتزاز الحر لتراكيب العتبة الميكانيكية المتضرره. في هذا البحث تم دراسة ثلاثة انواع من تراكيب العتبه والمسماة (العتبة البسيطة المدعمة beam simple supported والهيكل البابي portal frame والهيكل الرافعة crane frame). تم تمثيل الضرر بستة حالات في العتبة البسيطة المدعمة والهيكل البابي وسبعة حالات في الهيكل الرافعة. إن الضرر (Damage) يتمثل بتخفيض متانه العناصر المفترضة بنسبة 25 % و 50 % في وسط العتبة البسيطة وكذلك يتمثل عن طريق شق عمودي في العناصر المفترضة في المواقع المختلفة بنسبة عمق الشق إلى ارتفاع العتبة

0.25, 0.1 (a/h) للعتبة البسيطة و 0.2, 0.1 في الهيكل الباي والهيكل الرافعة. تم استخدام برنامج Matlab لتمثيل المحاكاة العددية لسينويوهات الضرر. اظهرت النتائج نقص في الترددات الطبيعية الخمسة وبوجود زحف في شكل النمط المتضرر damage mode shape نسبة للعتبة السليمه و الذي هو إشارة لوجود الضرر. تعطي المقارنة المباشرة إشارة الى وجود الضرر لكن موقع الضرر غير محدد. الطرق المحدده لايجاد الضرر التي تم استخدامها هي اربعة طرق مستندة على التغييرات في خصائص ديناميكة تراكيب العتبة و الطرق المحدده فحصت وقيمت حالات الضرر للتراكيب الثلاثة. نتائج التحليل تشير إلى ان طريقة دليل ضرر طاقة النغوس damage curvature- energy damage index هي الافضل في إكتشاف وتحديد مكان الضرر في سيناريوهات الضرر damage scenarios الوحيدة الموقع والمتعدّد المواقع للتراكيب الثلاثة.

KEYWORDS

Damage, Crack, Damage location, Curvature, Frame, Frequencies.

INTRODUCTION

The ability to monitor a structure and detect damage at the earliest possible stage is of outmost importance in mechanical, civil and aerospace engineering communities. Structural damage is considered as a weakening of the structure that negatively affects its performance. Damage may be also defined as any deviation in the structural original geometric or material properties that may cause undesirable stresses, displacements, or vibrations on the structure. These weakenings and deviation may be due to cracks, loose bolts, broken welds, corrosion, fatigue, etc. (Ren, 2002). Many structural components are now decaying because of age, deterioration, and lack of maintenance or repair.

Current nondestructive damage detection (NDD) technique are either visual or are based on experimental methods. Visual inspection has always been the most common method used in detecting damage in a structure, but the size and degree of complexity of today's structures being built provide less scope for visual inspections. The experimental methods such as acoustic or ultrasonic techniques, magnetic field procedure, radiography, eddy current, etc. All of these experimental methods require that the damaged region be identified a priori, and that the segment of the structure being examined must be easily accessible, subjected to these limitations, these methods can detect on or near the surface of the structure. The methods are obviously "local" inspection approaches (De wen, 2004).

One way to overcome the previously mentioned limitations is by using global damage detection methods. Structural damage identification based on changes in dynamic characteristics provides a global way to evaluate the structural condition. These methods are based on the idea that modal parameters (i.e., natural frequencies, mode shapes and modal damping ratio) are a function of the physical properties of the structure stiffness, damping, mass and boundary conditions (Herrera, 2005). Therefore, changes in the physical properties will cause detectable changes for the changes in the modal parameters.

MODELING THE STIFFNESS MATRIX OF THE CRACKED ELEMENT

It is assumed that the damage in the beam structure will affect only the stiffness matrix and not to the mass matrix. This assumption is consistent with those used by (Yuen 1985, Qian 1990 and Kisa 2000).

The beam is divided into elements and the behavior of the elements located to the right of the cracked element regarded as external forces applied to the cracked element, while the behavior of elements situated to its left as constraints, see Fig.1. Thus the flexibility matrix of a cracked element with constraints can be calculated. The strain energy of undamaged element in case of bending (Singor, 1951), is:



$$W^{(0)} = \int_0^L \frac{M_1^2 dx}{2EI} \quad (1)$$

As shown in **Fig. 1**,

$$M_1 = (px + M) \quad (2)$$

Substitute Eq. (2) in (1) to get

$$W^{(0)} = \int_0^L \frac{(px + M)^2}{2EI} dx \quad (3)$$

$$W^{(0)} = \frac{1}{2EI} \left[\frac{p^2 L^3}{3} + pML^2 + M^2 L \right] \quad (4)$$

Where:

$W^{(0)}$: The strain energy of undamaged element.

E : Elastic modulus.

I : Moment of inertia of undamaged element.

L : Length of the finite element.

p : Internal shear force at the right end of beam.

M : Internal bending moment at the right end of beam.

And by using the relation below, (**Thomson 1988**).

$$\{ u \} = [C] \{ P \} \quad (5)$$

$[C]$, $\{ u \}$, $\{ P \}$ are the influence coefficient flexibility matrix, displacement and force vectors, respectively.

The component of flexibility matrix $[C]$ can be written as, (**Thomson 1988**).

$$c_{ij} = \frac{\partial u_i}{\partial P_j} \quad (6)$$

And the displacement u_i computed by using Castigliano's theorem (**Singor, 1951**). As

$$u_i = \frac{\partial W^{(0)}}{\partial P_i} \quad (7)$$

Substitute Eq. (7) into (6), the flexibility coefficient of undamaged element evaluated as

$$C_{ij}^{(0)} = \frac{\partial^2 W^{(0)}}{\partial p_i \partial p_j} \quad (8)$$

where:

$$p_1 = p, p_2 = M \quad i, j = 1, 2$$

And using Eq. (4) in Eq. (8) gives:

$$C_{11} = \frac{\partial^2 W^{(0)}}{\partial p_1 \partial p_1} = \frac{\partial^2 W^{(0)}}{\partial p \partial p} = \frac{1}{2EI} \frac{\partial^2}{\partial p^2} \left[M^2 L + MpL^2 + \frac{p^2 L^3}{3} \right]$$

$$C_{11} = \frac{L^3}{3EI}$$

The flexibility matrix of the uncracked element can be expressed as

$$[C^{(0)}] = \frac{1}{EI} \begin{bmatrix} \frac{L^3}{3} & \frac{L^2}{2} \\ \frac{L^2}{2} & L \end{bmatrix} \quad (9)$$

From the equilibrium conditions shown in Fig (2), the following relationships hold:

$$\sum F_y = 0 \quad (10)$$

$$P_i + P_{i+1} = 0 \quad \text{or} \quad P_i = -P_{i+1} \quad (11)$$

$$\sum M_A = 0 \quad (12)$$

$$M_{i+1} + P_{i+1}L + M_i = 0 \quad (13)$$

$$M_i = -P_{i+1}L - M_{i+1} \quad (14)$$

From Eq. (11) and (14) we get in matrix form

$$\begin{Bmatrix} P_i \\ M_i \end{Bmatrix} = \begin{bmatrix} -1 & 0 \\ -L & -1 \end{bmatrix} \begin{Bmatrix} P_{i+1} \\ M_{i+1} \end{Bmatrix}$$

$$\begin{Bmatrix} P_i \\ M_i \\ P_{i+1} \\ M_{i+1} \end{Bmatrix} = \begin{bmatrix} -1 & 0 \\ -L & -1 \\ 1 & 0 \\ 0 & 1 \end{bmatrix} \begin{Bmatrix} P_{i+1} \\ M_{i+1} \end{Bmatrix}$$

$$\{P_i \quad M_i \quad P_{i+1} \quad M_{i+1}\}^T = [T] \{P_{i+1} \quad M_{i+1}\}^T \quad (15)$$

Where

$$[T] = \begin{bmatrix} -1 & -L & 1 & 0 \\ 0 & -1 & 0 & 1 \end{bmatrix}^T \quad (16)$$

The element stiffness matrix in base system is obtained by the inversion of the flexibility matrix as



$$[K] = [C]^{-1} \tag{17}$$

The stiffness matrix of undamaged element can be written as

$$[K_u] = [T] [C^{(0)}]^{-1} [T]^T \tag{18}$$

$$[K_u] = \frac{EI}{L^3} \begin{matrix} & \begin{matrix} u_i & \theta_i & u_{i+1} & \theta_{i+1} \end{matrix} \\ \begin{bmatrix} 12 & 6L & -12 & 6L \\ & 4L^2 & -6L & 2L^2 \\ & & 12 & -6L \\ sym & & & 4L^2 \end{bmatrix} & \begin{matrix} u_i \\ \theta_i \\ u_{i+1} \\ \theta_{i+1} \end{matrix} \end{matrix} \tag{19}$$

The stiffness matrix of undamaged element $[K_u]$ is the same that developed by (Merovitch 1975), for undamaged beam element with rectangular cross-section given by Bernoulli-Euler theory have two nodes with two degree of freedoms (2 d. o.f.s), $\{u, \theta\}$ at each node, as seen in Fig. 2, the mass matrix for an element without crack is

$$[M_u] = \frac{\bar{m}L}{420} \begin{matrix} & \begin{matrix} 156 & 22L & 54 & -13L \\ & 4L^2 & 13L & -3L^2 \\ & & 156 & -22L \\ sym & & & 4L^2 \end{matrix} \end{matrix} \tag{20}$$

Where \bar{m} is the mass per unit length.

According to the principle of Saint-Venant, the stress field is affected only in the region adjacent to crack. However, the calculation of the additional stress energy of a crack has been studied in fracture mechanics and the flexibility coefficient expressed by a stress intensity factor can be derived by applying the Castigliano's theorem in linear-elastic range.

From the condition of equilibrium, the stiffness matrix of the cracked element in the free-free state can be derived. For a rectangular beam having width b and height h the additional strain energy $W^{(1)}$ due to the crack, (Dewen 2004) can be written as

$$W^{(1)} = \int_0^{Ac} \frac{\partial W^{(1)}}{\partial A} dA = \int_0^{Ac} J dA \tag{21}$$

Where Ac is the area of the crack surface. The idea of relating J , strain energy release rate to the stress intensity factor K was proposed by (Hellan 1984) for the three modes, who gave the general formula of J as a function of stress intensity factor K as:

$$J = \frac{\beta}{E} K_I^2 + \frac{\beta}{E} K_{II}^2 + \frac{1+\nu}{E} K_{III}^2, \quad \beta = \begin{cases} 1 & \text{for plane stress} \\ 1-\nu^2 & \text{for plane strain} \end{cases} \quad (22)$$

Where K_I, K_{II}, K_{III} is the stresses intensity factors for fracture mode of I, II, III which are opening, sliding and tearing types respectively, and ν is the Poisson's ratio. The stress intensity factor K_i from (Hellan 1984) is:

$$K_i = \sigma_i \sqrt{\pi a} F(a/h) \quad (23)$$

Where σ_i is the stress for the corresponding fracture mode, a is the depth of the crack, $F(a/h)$ is the correction factor for the finite specimen.

Substituting Eq. (22) into Eq. (21) gives the additional strain energy due to the crack $W^{(1)}$

$$W^{(1)} = b \int_0^a \left(\frac{K_I^2 + K_{II}^2}{E_p} + \frac{(1+\nu)K_{III}^2}{E} \right) da \quad \text{where } dA = b \times da \quad (24)$$

$E_p = E$ For plane stress, $E_p = E/(1-\nu^2)$ for plane strain and b is the width of the beam.

The case of plane stress or plane strain, it depends on the dimensions of the beam, and this study take into account the plane stress since the beam is thin (slender) when the length is more than (10) times its least lateral dimensions (Singor 1951).

Taking into account only bending including the opening (I) and sliding (II) modes, the Eq. (24) becomes;

$$W^{(1)} = b \int_0^a \left\{ \left[(K_{IM} + K_{IP})^2 + K_{IIP}^2 \right] / E_P \right\} da \quad (25)$$

Where K_{IM}, K_{IP}, K_{IIP} are stress intensity factors for opening-type and sliding mode cracks due to M and P , respectively and by using Eq. (23)

$$K_{IM} = (6M/bh^2) \sqrt{\pi a} F_I(s) \quad \text{where} \quad \sigma = \frac{My}{I} = \frac{Mh/2}{bh^3/12} \quad (26)$$

$$K_{IP} = (3PL/bh^2) \sqrt{\pi a} F_I(s) \quad \text{where} \quad \sigma = \frac{My}{I} = \frac{PL/2 \cdot h/2}{bh^3/12} \quad (27)$$

$$K_{IIP} = (P/bh) \sqrt{\pi a} F_{II}(s) \quad \text{where} \quad \sigma = \frac{P}{A} = \frac{P}{bh} \quad (28)$$



Where $F_I(s)$ and $F_{II}(s)$ are the correction factors for crack mode I and mode II , ($s = a/h$) is defined as the ratio between the crack depth a and the height of the element h , the correction factor from (Kisa 2000) as

$$F_I(s) = \sqrt{(2/\pi s) \tan(\pi s/2)} \frac{0.923 + 0.199[1 - \sin(\pi s/2)]^4}{\cos(\pi s/2)} \quad (29)$$

$$F_{II}(s) = (3s - 2s^2) \frac{1.122 - 0.561s + 0.085s^2 + 0.18s^3}{\sqrt{1-s}} \quad (30)$$

And the additional flexibility coefficients due to the presence of the crack $C_{ij}^{(1)}$ are

$$C_{ij}^{(1)} = \frac{\partial^2 W^{(1)}}{\partial P_i \partial P_j} \quad (31)$$

$$P_1 = P, \quad P_2 = M, \quad i, j = 1, 2$$

Substituting Eq. (33) into Eq. (39) and integrate over the crack height, we get the coefficients $C_{ij}^{(1)}$ which can be expressed in matrix form as

$$[C^{(1)}] = \frac{b\pi a^2}{E_p} \begin{bmatrix} 9\beta_1^2 L^2 + \beta_2^2 & 18\beta_1^2 L \\ 18\beta_1^2 L & 36\beta_1^2 \end{bmatrix} \quad (32)$$

Where $\beta_1 = F_I(s)/bh^2$ and $\beta_2 = F_{II}(s)/bh$

The total flexibility coefficients C_{ij} for the element with an open crack are

$$C_{ij} = C_{ij}^{(0)} + C_{ij}^{(1)} \quad (33)$$

The total flexibility matrix $[C]$ for the element with an open crack can be expressed as

$$[C] = [C^{(0)}] + [C^{(1)}] \quad (34)$$

The stiffness matrix of the cracked element $[K_c]$ can be written as

$$[K_c] = [T][C]^{-1}[T]^T \quad (35)$$

With program coded in Maple 7, the coefficients of the stiffness matrix $[K_c]$ are calculated as :

$$[K_c] = \begin{bmatrix} k_{11} & k_{12} & k_{13} & k_{14} \\ k_{21} & k_{22} & k_{23} & k_{24} \\ k_{31} & k_{32} & k_{33} & k_{34} \\ k_{41} & k_{42} & k_{43} & k_{44} \end{bmatrix} \quad (36)$$

$$k_{11} = 12 \frac{EI E_p}{L^3 E_p + 12b\pi a^2 EI \beta_2^2}$$

$$k_{12} = 6 \frac{E_p EIL}{L^3 E_p + 12b\pi a^2 EI \beta_2^2}$$

$$k_{13} = -12 \frac{EI E_p}{L^3 E_p + 12b\pi a^2 EI \beta_2^2} = -k_{11}$$

$$k_{14} = 6 \frac{E_p EIL}{L^3 E_p + 12b\pi a^2 EI \beta_2^2}$$

$$k_{21} = k_{12}$$

$$k_{22} = 4 \frac{(L^3 E_p + 27b\pi a^2 EI \beta_1^2 L^2 + 3b\pi a^2 EI \beta_2^2) EI E_p}{(LE_p + 36b\pi \beta_1^2 a^2 EI)(L^3 E_p + 12b\pi a^2 EI \beta_2^2)}$$

$$k_{23} = -6 \frac{E_p EIL}{L^3 E_p + 12b\pi a^2 EI \beta_2^2}$$

$$k_{24} = 2 \frac{(L^3 E_p + 54b\pi a^2 EI \beta_1^2 L^2 - 6b\pi a^2 EI \beta_2^2) EI E_p}{(LE_p + 36b\pi \beta_1^2 a^2 EI)(L^3 E_p + 12b\pi a^2 EI \beta_2^2)}$$

$$k_{31} = k_{13} = -k_{12}$$

$$k_{32} = k_{23}$$

$$k_{33} = k_{11} = 12 \frac{EI E_p}{L^3 E_p + 12b\pi a^2 EI \beta_2^2}$$

$$k_{34} = -6 \frac{E_p EIL}{L^3 E_p + 12b\pi a^2 EI \beta_2^2} = -k_{14}$$

$$k_{41} = k_{14}$$

$$k_{42} = k_{24}$$

$$k_{43} = k_{34} = -k_{14}$$

$$k_{44} = 4 \frac{(L^3 E_p + 27b\pi a^2 EI \beta_1^2 L^2 + 3b\pi a^2 EI \beta_2^2) EI E_p}{(LE_p + 36b\pi \beta_1^2 a^2 EI)(L^3 E_p + 12b\pi a^2 EI \beta_2^2)} = k_{22}$$

Therefore:

$$[K_C] = \begin{bmatrix} k_{11} & k_{12} & -k_{11} & k_{14} \\ k_{12} & k_{22} & -k_{12} & k_{24} \\ -k_{11} & -k_{12} & k_{11} & -k_{14} \\ -k_{14} & k_{24} & -k_{14} & k_{22} \end{bmatrix} \quad (37)$$

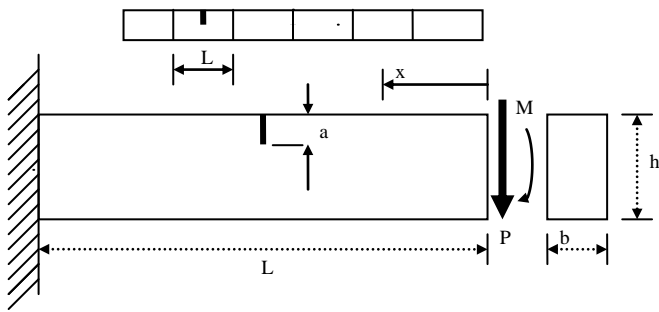


Fig.1: Diagram of a generic element

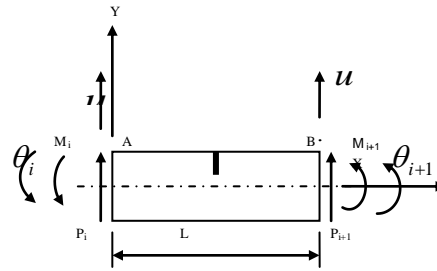


Fig. 2: Equilibrium condition of a generic element

FREE VIBRATION ANALYSIS AND DAMAGE DETECTION METHODS

EIGENVALUES AND EIGENVECTORS

For free vibration with undamped system, the equation of motion expressed by matrix form is

$$[M] \left\{ \ddot{x} \right\} + [K] \{x\} = \{0\} \tag{38}$$

Where:

K : Stiffness matrix of the system.

M : Mass matrix of the system.

$\{x\}$: Mode shape vector.

$$M \ddot{X} + KX = 0 \tag{39}$$

By using Eigen Value Problem algorithm EVP , the natural frequencies and mode shapes are obtained.

DAMAGE EFFECT ON MODAL PARAMETERS

Three structures of beam (simply supported and two plane frames: portal and crane frames) had been used to study the damage effect on modal parameters (frequencies and mode shapes).

- Simply Supported Beam

The free vibration of a simply supported beam with and without damage is performed. Modal responses of the beam are generated using finite element models before and after damaging episode cases. The dimensions and material properties of the simply supported steel beam are listed in **Table 1** and **Fig .3** illustrates the model of the simply supported beam.

For Finite Element Analysis purposes, the beam is divided into 40 elements. Here, six damage scenarios are investigated, as summarized in **Table 2**. In the first two cases (1, 2), the damage is simulated by reducing the stiffness of assumed elements. In cases (3 to 6), damage is simulated in the form of cracks. The finite element model of the beam uses the stiffness matrix of the cracked element described **Eq. (37)**.

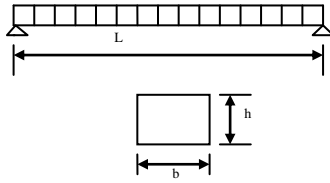


Fig.3: Simply supported beam

Table 1: Dimensions and material properties for beam

Length of the beam	$L = 254 \text{ cm.}$
Height of the cross section	$h = 10.16 \text{ cm.}$
Mass density	$\rho = 7808 \text{ kg/m}^3$
Width of the cross section	$b = 5.08 \text{ cm.}$
Elastic modulus	$E = 199.95 \text{ GPa.}$

Table 2: Damage scenario for simply supported beam

Damage scenario	Damaged Position	Stiffness Reduction (%)	Crack depth ratio a/h
D1	21~ (0.5L)	25	
D2	21~ (0.5L)	50	
C1	21~ (0.5L)		0.1
C2	21~ (0.5L)		0.25
C3	9~ (0.2 L), 21~ (0.5L)		0.1
C4	9~ (0.2 L), 21~ (0.5L)		0.25

- Portal Frame

The free vibration analysis of a portal frame with and without damage was performed. The modal quantities of the portal frame were numerically generated using finite element without and with damage episodes. The dimensions of the portal frame are listed in **Table 3**; **Fig 4** illustrates the model of the frame. For modal analysis purpose, the beam and the columns were divided into 40 elements. As in the case of the simply supported beam, the dynamic characteristic (frequencies and mode shapes) before and after the damage were calculated for each damage scenario in **Table 4**.

Table 3: Dimensions and material properties for portal frame

Length of the beam in the frame	$L = 243.84 \text{ cm}$
Column height	$H_c = 243.84 \text{ cm}$
Cross section width	$b = 5.08 \text{ cm}$
Cross section Height	$h = 12.7 \text{ cm}$
Mass density	$\rho = 7808 \text{ kg / m}^3$
Elastic modulus	$E = 199.95 \text{ GPa}$

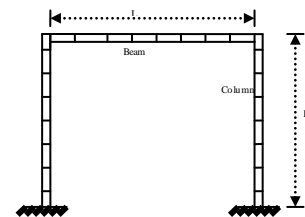


Fig.4: Portal frame

Table 4: Damage scenarios for portal frame.

Damage scenario	Damage member	Damaged position	a/h
PC1	Right column	4 (from col. base) ~ (0.1 L)	0.1
PC2	Right column	4 (from col. base) ~ (0.1 L)	0.2
PC3	Beam	21~ (0.5L)	0.1
PC4	Beam	21~ (0.5L)	0.2
PC5	Beam	21, 36 ~ (0.5L, 0.9L)	0.1
PC6	Beam	21, 36 ~ (0.5L, 0.9L)	0.2

- Crane Frame

The modal quantities of the crane frame were numerically generated using finite element without and with damage episodes. The dimensions and material properties of the crane frame are listed in **Table 5**, **Fig. 5** illustrates the model of the crane frame. For modal analysis purpose, the vertical column was divided into 40 elements while the horizontal column divided into 20 elements. Seven damage scenarios were investigated and are summarized in **Table 6**.

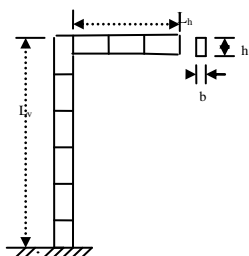


Table 5: Dimensions and material properties for crane frame

Vertical column	$L_v = 254$ cm
Horizontal column	$L_h = 127$ cm
Cross section width	$b = 5.08$ cm
Cross section Height	$h = 12.7$ cm
Elastic modulus	$E = 199.95$ GPa
Mass density	$\rho = 7808$ kg / m ³

Fig.5: Crane frame model

Table 6: Damage scenarios for crane frame

Damage scenarios	Damaged element	Damaged element	Damage severity a/h
C1	Vertical column	8 (from col.base)~ 0.2L	0.1
C2	Vertical column	8 (from col.base)~ 0.2L	0.2
C3	Vertical column	8,30~ (0.2L,0.75L)	0.1
C4	Vertical column	8,30~ (0.2L,0.75L)	0.2
C5	Horizontal column	10 ~ (0.5L)	0.1
C6	Horizontal column	10 ~ (0.5L)	0.2
C7	Horizontal column	10 ~ (0.5L)	0.5

DAMAGE DETECTION METHODS FOR BEAM STRUCTURES

In this research a different methods have been monitored here to detect damage in the beam structures which can be classified into two categories:

- Methods based on changes in mode shapes and frequencies.
 - **Eigenparameter method.**
 - **Mode shape relative difference method.**

- Methods based on the mode shape curvature.

A. Absolute difference curvature mode shape method.

B. Curvature-energy damage index method.

1. Methods Based on Changes in Mode Shapes and Frequencies

A. Eigenparameter Method

The eigenparameter method was proposed by (Yuen 1985) and (Salawe 1993) to detect the presence and location of damage in a cantilever beam. It is based on the premise that the mode displacements associated with each of the dynamic degrees of freedom would be affected differently by presence of damage and the changes in the mode shapes should reflect the location and extent of the damage.

$$([K] - \lambda_i [M]) \{\phi\}_i = 0 \quad (40)$$

$$([K^*] - \lambda_i^* [M]) \{\phi^*\}_i = 0 \quad (41)$$

A parameter that accounts for the changes in the frequencies and mode shapes of the structure is proposed to be used for damage detection. For the i -th mode shape, the eigenparameter is defined by

$$\{U\}_i = \frac{\{\phi^*\}_i}{\omega_i^{*2}} - \frac{\{\phi\}_i}{\omega_i^2} \quad (42)$$

λ_i : The eigenvalue, $\lambda_i = \omega_i^2$.

$\{U\}_i$: Eigenparameter vector.

$\{\phi\}_i$: Undamaged mode shape vector.

$\{\phi^*\}_i$: Damaged mode shape vector.

ω_i^2 : Undamaged eigenvalue.

ω_i^{*2} : Damaged eigenvalue.

B. Mode Shape Relative Difference Method.

In this formulation, a comparison of the displacement mode shapes is used as an indicator of the damage location. The parameter used is the relative difference (RD) between the mode shapes for the



undamaged and damaged structure. For the i -th mode shape the parameter is a vector defined as (Fox 1992):

$$\{RD\}_i = \frac{\{\phi\}_i - \{\phi^*\}_i}{\{\phi\}_i} \quad (43)$$

Where:

$\{\phi\}_i$: Normalized undamaged mode shape vector.

$\{\phi^*\}_i$: Normalized damaged mode shape vector.

In theory a plot of the vector $\{RD\}$ as a function of the measurement locations should show a definite trend with distinct discontinuity at the damage locations.

- Methods based on the mode shape curvature

A. Absolute Difference Curvature Mode Shape.

It has been evaluated by (Pandy 1991) and (Shakkar 2006). Curvature mode shape is related to the flexural stiffness of the beam cross-sections. By definition, (Black 1966), the curvature at a point of an element with bending deformation, is given by:

$$v'' = \frac{M}{EI} \quad (44)$$

In which v'' is the curvature at a section, M is the bending moment at a section, E is the modulus of elasticity and I is the second moment of the cross-sectional area.

If crack or other damage is introduced in a structure, it reduces the flexural stiffness EI of the structure at the cracked section in the damaged region. This in turn increases the magnitude of curvature at that section of the structure. The change in the curvature increases with the reduction in the value of the flexural stiffness EI .

Starting with the displacement mode shapes obtained from the finite element analysis, the curvature mode shapes for the undamaged structure can be obtained numerically using a central difference approximation as

$$\phi_i'' = \frac{\phi_{i-1} - 2\phi_i + \phi_{i+1}}{H^2} \quad (45)$$

Where:

H : Distance between the measurement points (i) and ($i+1$).

ϕ_i : Mass normalized mode shape of the undamaged structure associated with a given frequency.

Similarly, the curvature mode shape for the damaged structure can be obtained as

$$\phi_{*,i}'' = \frac{\phi_{i-1}^* - 2\phi_i^* + \phi_{i+1}^*}{H^2} \quad (46)$$

Where,

ϕ_i^* : Mass normalized mode shape of the damaged structure corresponding to specific natural frequency.

For mode j the absolute difference between the curvatures of the damaged and undamaged structure is calculated as

$$\{\Delta\phi''\}_j = |\{\phi_*''\}_j - \{\phi''\}_j| \quad (47)$$

B. Curvature-Energy Damage Index Method

The presence of the damage in a beam structure increases the magnitude of the curvature at that section of the structure. In this section a damage index based on the modal curvature is proposed by (Herrera 2005). It is based on the concept of the pseudo flexibility matrix. The proposed modal curvature-energy based matrix can be defined by

$$[X]_{n \times n} = [\Phi'']_{n \times m} [\Lambda]_{m \times m}^{-1} [\Phi'']_{m \times n}^T \quad (48)$$

Where n the number of points for mode is shape measurement and m is the number of measured modes. $[\Phi'']$ Is the modal curvature matrix formed by the curvature mode shapes $\{\phi_i''\}$:

$$[\Phi''] = [\{\phi_1''\} \quad \{\phi_2''\} \quad \dots \quad \{\phi_m''\}] \quad (49)$$

$[\Lambda]$: Matrix contains diagonal Eigenvalues.

For the damaged structure, the proposed curvature-energy matrix can be expressed as

$$[X^*]_{n \times n} = [\Phi_*'']_{n \times m} [\Lambda]_{m \times m}^{-1} [\Phi_*'']_{m \times n}^T \quad (50)$$

For the undamaged structure, the corresponding curvature-energy matrix is given by Eq. (48). In terms of these curvature-energy matrices, the relationship between damaged and undamaged states, is defined by

$$\{x\} = \{x_*\} ./ \{x_u\} \quad (51)$$

Where the symbol $./$ is used to indicate that the division of the vectors is done by element.

$\{x_u\}$: Diagonal of matrix $[X]$.

$\{x_*\}$: Diagonal of matrix $[X^*]$.

It is proposed to define the damage index for the j th location as

$$k_j = |x_j - 1| \quad (52)$$



RESULTS AND DISCUSSION

The Results and Discussion for Simply Supported Beam

The results for the first five frequencies are listed in **Table 7** for the damage scenarios considered in **Table 2** for simply supported beam.

Table 7: Natural frequencies of the simply supported beam

Damage Scenario	Natural Frequency (rad/sec)				
	Mode 1	Mode 2	Mode 3	Mode 4	Mode 5
Exact undamaged	227.0616	908.7063	2.0452×10^3	3.6329×10^3	5.6764×10^3
Present undamaged	227.0525	908.2102	2.0435×10^3	3.6329×10^3	5.6764×10^3
D1	225.1870	908.1489	2.0272×10^3	3.6319×10^3	5.6331×10^3
D2	221.5876	908.0297	1.9969×10^3	3.6301×10^3	5.5558×10^3
C1	226.3955	908.198	2.0377×10^3	3.6328×10^3	5.6609×10^3
C2	222.2865	894.2703	2.0027×10^3	3.6177×10^3	5.5702×10^3
C3	225.9728	905.0045	2.0286×10^3	3.6300×10^3	5.6540×10^3
C4	211.5363	875.7897	1.9674×10^3	3.5918×10^3	5.5540×10^3

The Results and Discussion for Portal Frame and Crane Frame

The results for the first five natural frequencies are listed in **Table 8** for the damage scenarios considered in **Table 4** for portal frame. It can be noted that the highest variation for the first modal frequency caused by simulated damage (crack) scenario was 0.46% and the highest decreasing for mode 2, 3, 4 and 5 were 0.99, 0.26, 1.1 and 0.18 %, respectively. It can be noted that the highest variation for the damage scenarios from C1 to C6 for the first modal frequency caused by simulated damage scenario was 2 % and the highest decreasing for mode 2, 3, 4 and 5 were 1.44, 0.33, 6.3 and 9.4 %, respectively for crane frame as in **Table 9**.

Table 8: Natural frequencies for portal frame

Damage Scenario	Natural Frequency (rad/sec)				
	Mode 1	Mode 2	Mode 3	Mode 4	Mode 5
Undamaged	101.9480	394.4309	653.5440	699.6075	1.3341×10^3
PC1	101.8173	393.7627	653.4660	698.1770	1.3269×10^3
PC2	101.4750	392.7021	653.4069	695.7772	1.3218×10^3
PC3	101.9471	393.4324	653.3958	698.2410	1.3339×10^3
PC4	101.9456	390.5907	653.0997	696.3602	1.3338×10^3
PC5	101.8433	393.3805	653.0262	696.3385	1.3334×10^3
PC6	101.5538	390.4968	651.8200	691.6682	1.3317×10^3

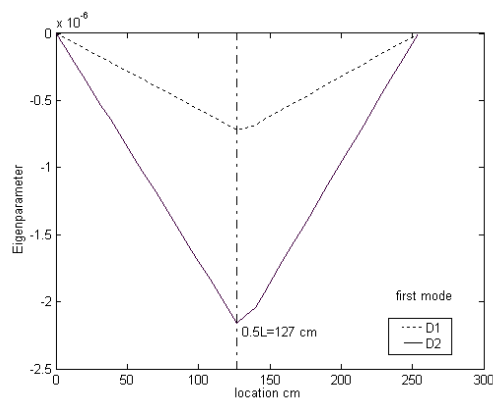
Table 9: Natural frequencies for Crane frame

Damage Scenarios	Natural Frequency (rad/sec)										
	Mode 1	Mode 2	Mode 3	Mode 4	Mode 5						
Undamaged	54.6114	221.3366	644.4290	1.5358×10^3	1.7672×10^3						
C1	54.3582	221.0727	644.0045	1.4969×10^3	1.6594×10^3						
C2	53.6443	220.6903	643.6281	1.4762×10^3	1.6363×10^3						
C3	54.2939	220.3281	643.4483	1.4710×10^3	1.6362×10^3						
C4	53.5103	218.1355	642.2623	1.4376×10^3	1.6010×10^3						
C5	54.5648	221.1289	643.7407	1.5301×10^3	1.7644×10^3						
C6	54.5630	220.7885	642.3609	1.5150×10^3	1.7596×10^3 </tr <tr> <td>C7</td> <td>54.5612</td> <td>215.3734</td> <td>621.4992</td> <td>1.3088×10^3</td> <td>1.7232×10^3</td> </tr>	C7	54.5612	215.3734	621.4992	1.3088×10^3	1.7232×10^3
C7	54.5612	215.3734	621.4992	1.3088×10^3	1.7232×10^3						

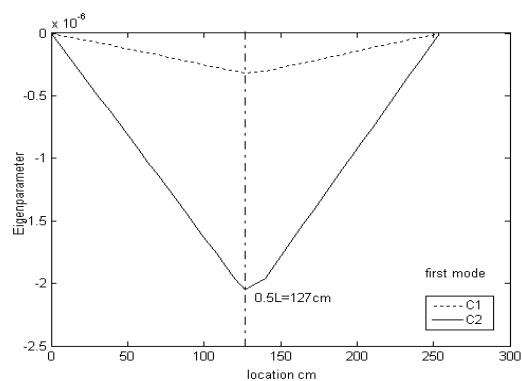
The Results and Discussion of Damage Detection Method

The Results and Discussion of Eigenparameter

The eigenparameter was calculated for the first two mode shapes. The parameter for the first mode shows the largest change at this location of the damage, i.e. the peak value occurs in the damaged region. Also at the location the slope changes sign. The damage scenarios D1, D2, C1 and C2 correspond to a single crack at the mid-span for simple beam. It can be observed that the absolute value of the parameter increases with an increase in the severity of the damage. The peak observed in **Fig .6** for single damage as in (a) and (b). For multiple damage, the peak is clear for one location of damage for portal frame and crane frame in **Fig .6**, for (c) and (d) for cases PC5, PC6 for portal frame and C3, C4 for crane frame respectively.



(a)



(b)

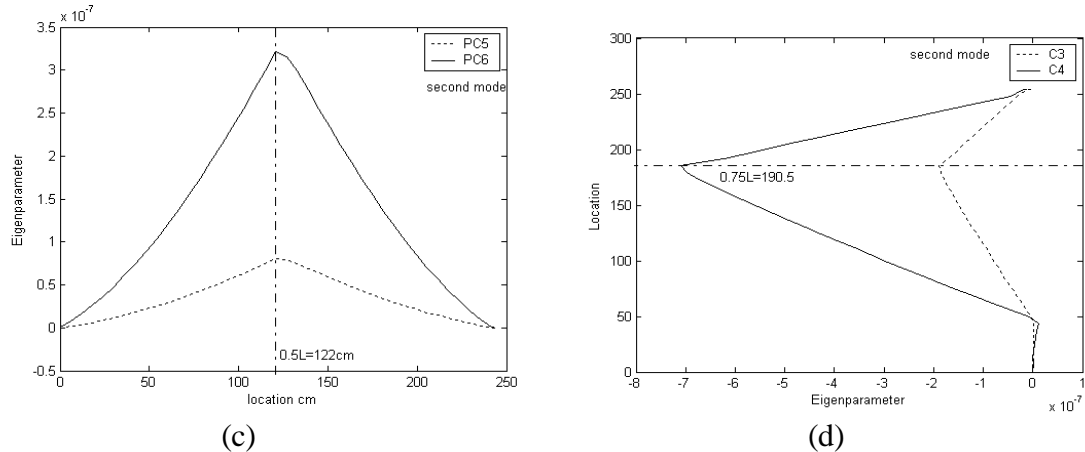
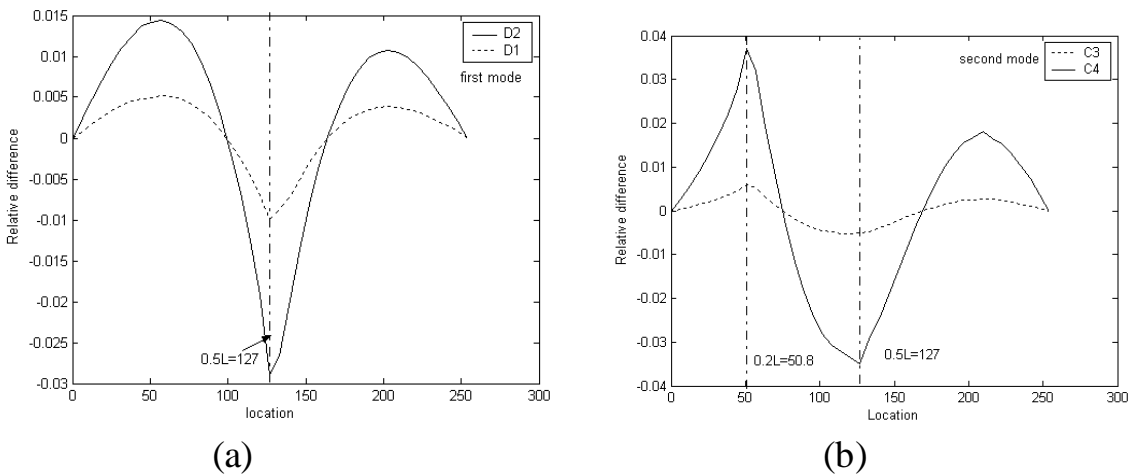
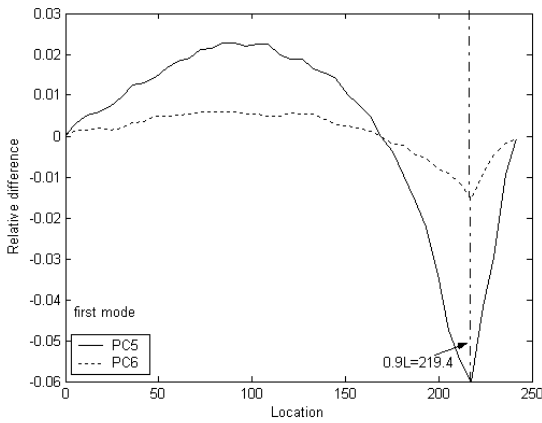


Fig. 6: Eigenparameter for 1st and 2nd modes of the simply supported beam (a, b), portal (c) and crane frames (d).

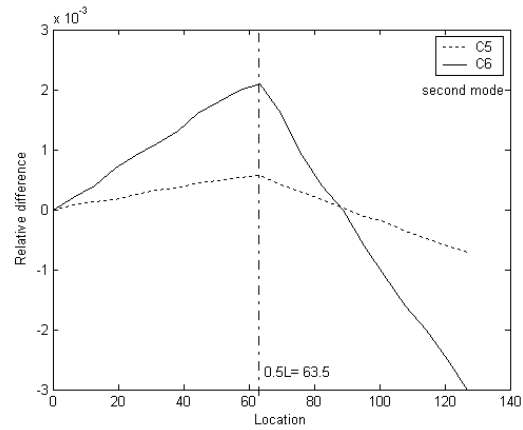
The Results and Discussion of Relative Difference Method

The peaks occur at damage location in **Fig. 7** for simply supported in (a) for single damage and (b) for multiple damage. The peak observed for one location for portal frame as in (c) and it's observed in (d). In Figures illustrated the mode difference was normalized with respect to the maximum absolute value of the mode shape of the undamaged system as in previous sections in simply supported, portal frame and crane frame. As expected, the differences are larger for case damage C2, since this correspond to a larger crack depth for the same cross section.





(c)

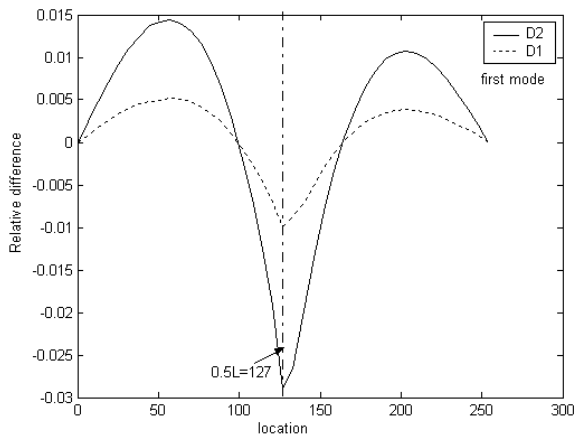


(d)

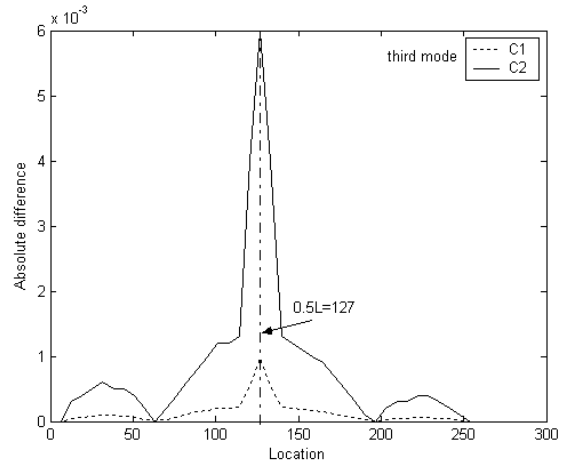
Fig. 7: Relative difference for first and second modes of the simply supported beam (a, b), portal (c) and crane frames (d).

The Results and Discussion for Absolute Difference Curvature Mode Shape

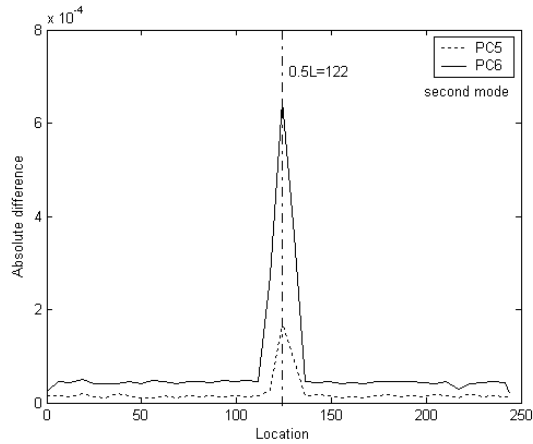
Fig. 8 Shows the results for damage scenarios D1, D2, C1, C2 for simple beam, PC5, PC6 for portal frame and C5, C6 for crane frame. As it can be seen in **Fig. 8**, the maximum difference for each curvature mode shape occurs in the damaged region, which is at location $0.5L$ for these damage scenarios. In the multiple damage scenarios (C3 and C4), the presence of two cracks at the vertical column is simulated. The defects are at position $(0.2L=50.8\text{cm}$ and $0.75L=190.5\text{cm})$ measured from the fixed end of the column. It is evident from the graphs displayed that the peak observed in the damage location as in (a), (b), (c) and (d).



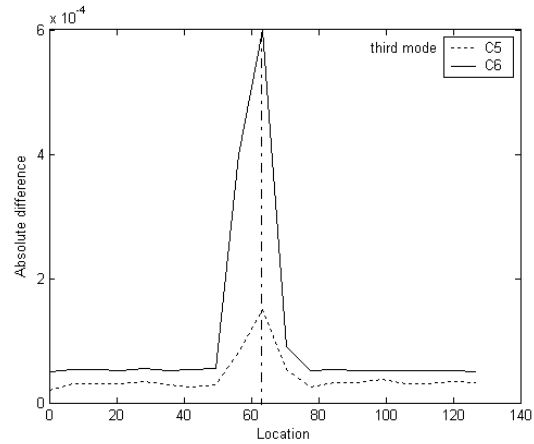
(a)



(b)



(c)

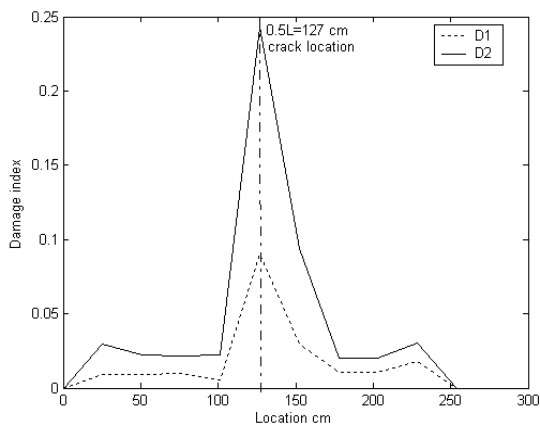


(d)

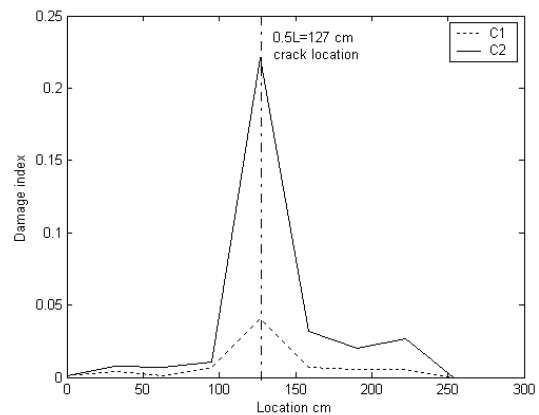
Fig. 8: Absolute difference curvatures for the three modes of the simply supported beam (a, b), portal frame (c) and crane frame (d).

The Results and Discussion of Curvature-Energy Damage Index Method

The results of the proposed damage index for the damage scenarios D1 to C4 are shown in **Fig. 9** is calculated using only two curvature mode shapes. When two cracks are induced in the beam (damage scenarios C3 and C4), the proposed method is capable of detecting the location of the two cracks, as evidenced by the peaks in the index k_j in **Fig 9**.



(a)



(b)

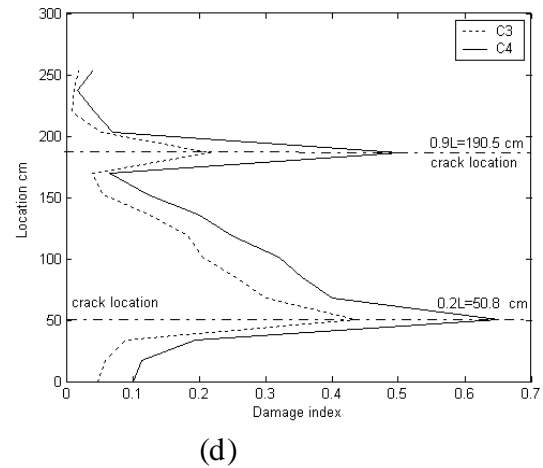
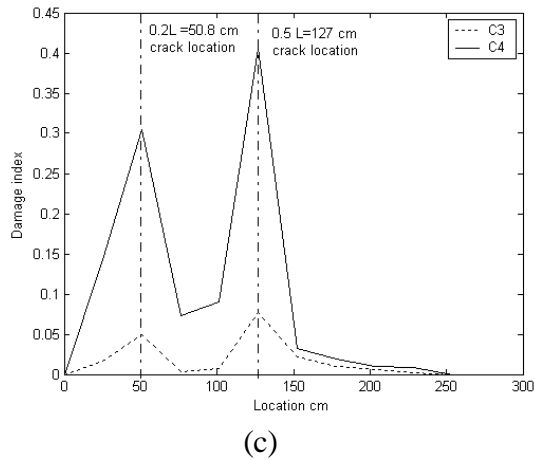


Fig. 9: Curvature-Energy damage index method for the three modes of the simply supported beam (a, b), portal frame (c) and crane frame (d).

CONCLUSION

The main conclusions from the present work according to the adopted data may be stated as follows:

- Based on assumption that the damage will change the stiffness reduction only and the mass of the beam be consistent, the increased severity of the damage will decrease the frequencies of the damaged beam.
- It's observed that, the damage representation as stiffness reduction 25% is not equal to the damage represented by crack ratio 25%, accordingly it's obvious that the crack is more sensitive than stiffness reduction in representing the damage.
- Changes on mode shape are much more sensitive to local damage when compared with changes in natural frequencies. However, using mode shapes also has some limitations, as the damage is a local phenomenon, it may not significantly influence the mode shapes of the lower modes, that are usually those measured from vibration tests, and it's obvious in large structures, as in portal frame.
- The structural damage identification technique based on changes in the displacement mode shapes, referred to eigenparameter was able to indicate the location of damage with only one crack in the three structures. For multiple damage scenarios, the eigenparameter was not locating the damage zones.
- The methodologies based on the modal curvatures energy exhibited superior performance in detecting and locating the damage. The curvature- energy damage index method is the best method used since; it does detect and locate the single or multiple damage in the three structures which considered in this study.



REFERENCES

- Black, P., (1966). “Strength of materials” /first edition.
- Dewen, B. E, M.E. (2004). “Damage detection in mechanical structures through coupled response measurements”. A thesis submitted in partial fulfillment of the requirements for the degree of Doctor of Philosophy in Mechanical Engineering /University of Queensland, Brisbane, Australia.
- Fox, C. H.J. (1992). “The location of defects in structures: A comparison of the use of natural frequency and mode shape data”. Proceeding of the 10th international modal analysis conference, San Diego, USA, P.522-528.
- Hellan, K., (1984). “Introduction to fracture mechanics”, (Book). University of Trondheim /Norway. Printed in USA.
- Herrera, J. C., (2005). “Evaluation of structural damage identification methods based on dynamic characteristics”. A thesis submitted in partial fulfillment of the requirements for the degree of Doctor of Philosophy in civil engineering / University of Puerto Rico.
- Kisa, M. and Brandon, J., (2000). “The effect of cracks on the dynamics of a cracked cantilever beam”. Available online at [http:// www.idealibrary.com](http://www.idealibrary.com) on **IDEAL**, Cardiff, England.
- Academic pressRen, W. X. and De Roeck, G. (2002). “Structural damage identification using modal data. I.: Simulation verification”. *ASCE*. Journal of structural engineering, Vol. 128, No. 1 January, 87-95.
- Merovitch L., (1975). “Elements of vibrations analysis”, (Book) International student edition.
- Pandey, A.K., Biswas, M. and Samman, M.M., (1991). “Damage detection from changes in curvature mode shapes ”.
- Qian, G.L. and Jiang, J.S., (1990) “The dynamic behavior and crack detection of a beam with a crack”. Journal of sound and vibration, Vol.138, No. 2, 233-243.
- Singor L., F., (1951). “Strength of materials”. Second edition (book).
- Thakkar, S. K., Ghoh, G. and Singh Y., (2006). “Structural damage identification and health monitoring and damage identification of bridges”. Journal. Advance in bridge engineering, March 24-25.
- Thomson, W.T, (1988). “Theory of vibration with applications”. Book / third edition. University of California, USA, printed in London.

- Yuen, M., (1985). "A numerical study of the eigenparameters of a damaged cantilever". Journal of sound and vibration, Vol. 103, No.3, 301-310.
- Salawe, O.S. and Williams, C. (1993). "Structural damage detection using experimental model analysis". Proceeding of the 11th international modal analysis conference, Kissimmee, Florida, 254-260.